VOLUME 123, NUMBER 20
MAY 23, 2001

JOURNAL OF THE AMERICAN CHEMICAL SOCIETY

Hybridization between Oxy-Peptide Nucleic Acids and DNAs: Dependence of Hybrid Stabilities on the Chain-Lengths, Types of Base Pairs, and the Chain Directions

Masayasu Kuwahara, Miki Arimitsu, Masanori Shigeyasu, Naho Saeki, and Masahiko Sisido*

Contribution from the Department of Bioscience and Biotechnology, Faculty of Engineering, Okayama University, 3-1-1 Tsushimanaka, Okayama 700-8530, Japan

Received November 6, 2000

Abstract: Oxy-peptide nucleic acids (OPNAs) of [-NH-CH(CH_2-CH_2-Base)-CH_2-O-CH_2-CO-]-type main chain with four different types of nucleobases (Base = A, G, C, and U) or with an abasic side group (X) were synthesized. Melting curves of the 1:1 hybrids of o(A_n)−d(T_n) pairs with n = 6, 9, 12, and 15 showed very sharp transitions at high T_m values, particularly for long chains, indicating that nearly optimum matching is attained in the structure of the o(A_n)−d(T_n) hybrids. Effect of different types of base pairs on the hybrid stabilities was examined for the o(A_4NA_4)−d(T_4N′T_4) 1:1 mixtures where N is A, G, C, U, or X and N′ is A, G, C, or T. In all series of the hybrids the complementary pairs showed the highest T_m values. The T_m values of the complementary pairs were about 35 °C when purine bases were inserted as the N group in the OPNA, but they were 20−23 °C when pyrimidine bases were inserted. The melting curves of the hybrids with a single mismatch were similar to those with a single X−N′ pair, suggesting that the mismatch base pairs have been ignored in the hybrids. All complementary OPNA−DNA hybrids showed higher T_m values and sharper transitions than the corresponding DNA−DNA hybrids. The OPNA−DNA hybrids favor a parallel direction i.e., the N-terminal of OPNA is directed to the 5′-terminal of DNA.

The rapid accumulation of the genomic information is urging chemists to develop artificial substances that selectively bind to a specific sequence on a gene. Among a variety of attempts, peptide nucleic acids (PNAs) developed by Nielsen's group have been attracting much interest,[1] because they can hybridize selectively to the complementary DNAs to form double-stranded or triple-stranded hybrids. Because of this unique property, PNAs have been finding applications as antisense drugs, as diagnostic devices, and as general biochemical tools.[2] PNAs consist of δ-amino acids with different nucleobases on the side chain. The δ-amino acids are linked together by conventional solid-phase peptide synthesis to obtain PNAs of specific base sequences.

After the success of Nielsen's PNA, analogous amino acids and their oligopeptides have been reported by a number of workers, and their hybridization with DNAs were examined.[3] These works are aiming to improve drawbacks of the Nielsen-

* Correspondence should be addressed to this author: Department of Bioscience and Biotechnology, Faculty of Engineering, Okayama University, 3-1-1 Tsushimanaka, Okayama 700-8530, Japan. E-mail: sisido@cc.okayama-u.ac.jp.

(1) (a) Nielsen, P. E.; Egholm, M.; Berg, R. H.; Buchardt, O. *Science* **1991**, *254*, 1497. (b) Egholm, M.; Buchardt, O.; Christensen, L.; Behrens, C.; Freier, S. M.; Driver, D. A.; Berg, R. H.; Kim, S. K.; Nordén, B.; Nielsen, P. E. *Nature* **1993**, *365*, 566. (c) Wittung, P.; Nielsen, P. E.; Buchardt, O.; Egholm, M.; Nordén, B. *Nature* **1994**, *368*, 561. (d) Bohler, C.; Nielsen, P. E.; Orgel, L. E. *Nature* **1995**, *376*, 578. (e) Veselkov, A. G.; Demidov, V. V.; Frank-Kamenetiskii, M. D.; Nielsen, P. E. *Nature* **1996**, *379*, 214.

10.1021/ja003881i CCC: $20.00
Published on Web 04/28/2001

type PNAs, especially of purine-rich sequences. Usually the purine-rich PNAs show limited solubility in water and sometimes are difficult to synthesize. Another potential disadvantage of the Nielsen-type PNAs is their preference to form triplex rather than duplex. However, thus far, only very few of the new versions successfully hybridized to DNAs,[4] indicating that the main-chain and the side-chain structures of the oligopeptides must be very precisely matched to the DNA structures.

We have shown that another type of oligopeptide with side-chain adenine bases, [-NH-CH(CH_2-CH_2-A)-CH_2-O-CH_2-CO-]$_n$, also hybridizes with d(T_n) and we named the oligopeptide as oxy-peptide nucleic acid [OPNA or simply o(base sequence)].[5] The most notable advantage of the OPNA over the Nielsen-type PNA is the very sharp melting curve of the OPNA−DNA hybrids. In the case of the o(A_{12})−d(T_{12}) hybrid, for example, the temperature range for a 5−95% transition was 13 °C. This temperature range is much smaller than the corresponding hybrid of the Nielsen-type PNA(A_{12}) (30 °C). The melting temperature (T_m) of the o(A_{12})−d(T_{12}) hybrid (45 °C) is higher than that of the d(A_{12})−d(T_{12}) hybrid (30 °C) but lower than that of the PNA(A_{12})−d(T_{12}) hybrid (55 °C). Another advantage of OPNA is its improved solubility, particularly for the purine-rich sequences.

Syntheses of the OPNA monomers that carry five different nucleobases (A, G, C, U, and T) have been reported.[6] In this study, OPNAs of purine-rich mixed sequences were synthesized from the OPNA monomers and from an abasic[7] monomer [H_2N-CH(CH_3)-CH_2-O-CH_2-COOH]. Stabilities of the OPNA−DNA hybrids were studied for different chain lengths and for different combinations of the base pairs to clarify the nature of the OPNA−DNA hybrids in detail. Furthermore, the preferred chain direction in the OPNA−DNA hybrids was determined.

Experimental Section

The OPNA monomers, i.e., δ-amino acids that carry four different nucleobases (A, C, G, and U), have been synthesized as before.[5] As for the adenine monomer, however, the OPNA monomer with an unprotected adenine was used instead of the N-benzoyladenine derivative reported before. It was found that virtually no side reaction took place during the peptide synthesis with the unprotected adenine monomer as one component. The abasic OPNA monomer, H_2N−CH(CH_3)−CH_2−O−CH_2−COOH (X), was synthesized as described in the Supporting Information.

The common structure of the OPNAs used in this study is:

$$H[NHC^*H(CH_2CH_2Base)CH_2OCH_2CO]_nLys-NH_2$$

A lysine unit was attached at the C-terminal to increase the affinity to DNA. The peptide synthesis was carried out by using an Fmoc-NH−SAL-PEG resin (superacid-labile poly(ethylene glycol) resin, Watanabe Chemicals, Hiroshima, Japan) as the support, with benzotriazole-1-yl-oxy-tripyrrolidinephosphonium hexafluorophosphate (PyBop)/HOBt as the coupling reagents. After cleavage from the resin, the crude OPNA was purified by preparative HPLC (C18 column) to obtain a single peak in analytical HPLC. The sample was finally identified by a TOF-Mass spectroscopy (PE Biosystems, Voyager DE Pro). Details of the peptide synthesis are described in the Supporting Information. Oligo-DNAs were purchased from Lifetech Oriental Inc. (Tokyo, Japan).

UV and CD spectra were recorded on a Jasco Ubest 55 and on a Jasco J720WI instrument, respectively. The sample temperature was monitored by a thermocouple that was directly inserted into the cuvette and controlled by a Jasco ETC505 temperature controller. The solution in the cuvette was gently stirred during the measurement.

Results and Discussion

Chain-Length Dependence of the Melting Behavior of o(A_n)−d(T_n) Hybrids. A 1:1 hybridization has been observed for the o(A_{12})−d(T_{12}) pair.[5] To understand the nature of the hybrid in more detail, the melting curves of equimolar mixtures of o(A_n) and d(T_n) with different numbers of base pairs, $n = 6$, 9, 12, and 15, were measured. As has been reported for the $n = 12$ case, the melting curves on heating were essentially the same as the association curves on cooling for all chain lengths examined. The melting curves on heating are shown in Figure 1. All melting curves show very sharp transitions. The T_m values (and the temperature ranges for the 5−95% change) were 14 °C (∼23 °C) for $n = 6$, 35 °C (15 °C) for $n = 9$, 45 °C (13 °C) for $n = 12$, and 51 °C (10 °C) for $n = 15$. These values are compared with that of the d(A_{12})−d(T_{12}) hybrid, 30 °C (18.5 °C), and those of the Nielsen-type PNA(A_n)−d(T_n) hybrid, 24 °C (∼27 °C) for $n = 6$, 50 °C (24 °C) for $n = 9$, and 55 °C (30 °C) for $n = 12$. The sharp melting curves of the OPNA−DNA hybrids are advantageous in detecting mismatches in base sequences.

Thermodynamic parameters were calculated from the melting curves. The van't Hoff plots of the melting curves are shown in the inset of Figure 1. They were practically linear, except for the case of $n = 6$ for which some uncertainty remains in taking the low-temperature-side baseline. The enthalpy change and the entropy change were obtained from the van't Hoff plots and are listed in Table 1. Both the stabilization energy ($-\Delta H/n$) and the entropy loss ($-\Delta S/n$) per monomer unit remained unchanged, irrespective of the number of base pairs. This indicates that the structures of the A-T pairs are essentially

(2) (a) Nielsen, P. E.; Egholm, M.; Berg, R. H.; Buchardt, O. *Anti-Cancer Drug Des.* **1993**, *8*, 53. (b) Hanvey, J. C.; Peffer, N. J.; Bisi, J. E.; Thomson, S. A.; Cadilla, R.; Josey, J. A.; Ricca, D. J.; Hassman, C. F.; Bonham, M. A.; Au, K. G.; Carter, S. G.; Bruckenstein, D. A.; Boyd, A. L.; Noble, S. A.; Babiss, L. E. *Science* **1992**, *258*, 1481. (c) Wittung, P.; Kajanus, J.; Edwards, K.; Nielsen, P. E.; Norden, B.; Malmstrom, B. G. *FEBS Lett.* **1995**, *365*, 27 and *375*, 27 (d) Demidov, V. V.; Potaman, V. N.; Frank-Kamenetskii, M. D.; Egholm, M.; Buchard, O.; Sonnichsen, S. H.; Nielsen, P. E. *Biochem. Pharmacol*. **1994**, *48*, 1310. (e) Nielsen, P. E. *Bioorg. Med. Chem*. **1996**, *4*, 5. (f) Boado, R. J.; Tsukamoto, H.; Pardridge, W. M. *J. Pharm. Sci*. **1998**, *87*, 1308. (g) Branden, L. J.; Mohamed, A. J.; Edvard Smith, C. I. *Nature Biotechnol*. **1999**, *17*, 784. (h) Lohse, J.; Dahl, O.; Nielsen, P. E. *Proc. Natl. Acad. Sci. U.S.A.* **1999**, *96*, 11804. (i) Verheijen, J. C.; van der Marel, G. A.; van Boom, J. H.; Bayly, S. F.; Player, M. R.; Torrence, P. F. *Bioorg. Med. Chem*. **1999**, *7*, 449. (j) Hamilton, S. E.; Simmons, C. G.; Kathiriya, I. S.; Corey, D.R. *Chem. Biol*. **1999**, *6*, 343. (k) Mologni, L.; Nielsen, P. E.; Gambacorti-Passerini, C. *Biochem. Biophys. Res. Commun*. **1999**, *264*, 537.

(3) (a) Almarsson, O.; Bruice, T. C.; Kerr, J.; Zuckermann, R. N. *Proc. Natl. Acad. Sci. U.S.A.* **1993**, *90*, 7818. (b) Hyrup, B.; Egholm, M.; Nielsen, P. E.; Wittung, P.; Nordén, B.; Buchardt, O. *J. Am. Chem. Soc*. **1994**, *116*, 7964. (c) Tsantrizos, Y. S.; Lunetta, J. F.; Boyd, M.; Fader, L. D.; Wilson, M.-C. *J. Org. Chem*. **1997**, *62*, 5451. (d) Ciapetti, P.; Soccolini, F.; Taddei, M. *Tetrahedron* **1997**, *53*, 1167. (e) Lowe, G.; Vilaivan, T. *J. Chem. Soc., Perkin Trans. 1* **1997**, *4*, 539 (f) Efimov, V. A.; Choob, M. V.; Buryakova, A. A.; Kalinkina, A. L.; Chakhmakhcheva, O. G. *Nucleic Acids Res*. **1998**, *26*, 566.

(4) (a) Gangamani, B. P.; Kumar, V. A.; Ganesh, K. N. *Tetrahedron* **1996**, *52*, 15017. (b) Jordan, S.; Schwemler, C.; Kosch, W.; Kretschmer, A.; Stropp, U.; Schwenner, E.; Mielke, B. *Bioorg. Med. Chem. Lett*. **1997**, *7*, 687. (c) Wittung, P.; Nielsen, P. E.; Norden, B. *J. Am. Chem. Soc*. **1997**, *119*, 3189. (d) Fujii, M.; Yoshida, K.; Hidaka, J.; Ohtsu, T. *Chem. Commun*. **1998**, 717. (e) Barawker, D. A.; Kwok, Y.; Bruice, T. W.; Bruice, T. C. *J. Am. Chem. Soc*. **2000**, *122*, 5244. (f) Schultz, R.; Cantin, M.; Roberts, C.; Greiner, B.; Uhlmann, E.; Leuman, C. *Angew. Chem., Int. Ed*. **2000**, *39*, 1250. (g) García-Echeverría, C.; Hüsken, D.; Chiesi, C. S.; Altmann, K.-H. *Bioorg. Med. Chem. Lett*. **1997**, *7*, 1123. (h) Altmann, K.-H.; Hüsken, D.; Cuenoud, B.; García-Echeverría, C. *Bioorg. Med. Chem. Lett*. **2000**, *10*, 929. (i) Vilaivan, T.; Khongdeesameor, C.; Harnyuttanakorn, P.; Westwell, M. S.; Lowe, G. *Bioorg. Med. Chem. Lett*. **2000**, *10*, 2541. (j) Puschl, A.; Tedeschi, T.; Nielsen, P. E. *Org. Lett*. **2000**, *2*, 4161.

(5) Kuwahara, M.; Arimitsu, M.; Sisido, M. *J. Am. Chem. Soc*. **1999**, *121*, 256.

(6) Kuwahara, M.; Arimitsu, M.; Sisido, M. *Tetrahedron* **1999**, *55*, 10067.

(7) Challa, H.; Woski, S. A. *Tetrahedron Lett*. **1999**, *40*, 8333.

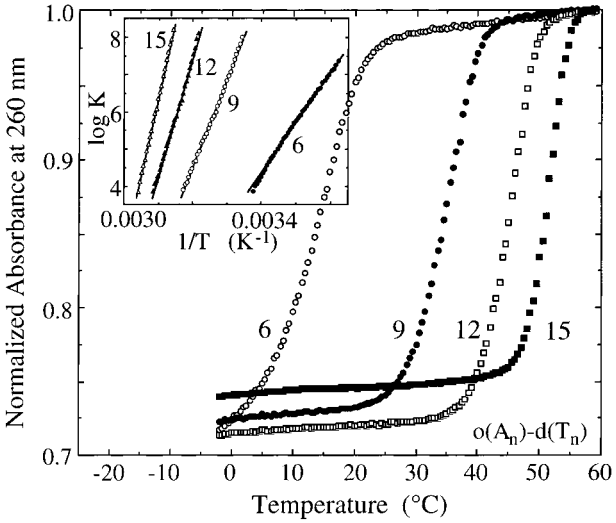

Figure 1. Temperature dependence of absorption intensity at 260 nm for equimolar mixtures of o(A_n)−d(T_n) with n = 6, 9, 12, and 15, in 100 mM NaCl, 10 mM NaH_2PO_4 and 0.1 mM EDTA, pH 7.0. [A_n] = [T_n] = 5×10^{-6} M. The melting curves were recorded with heating the solution at 0.5 °C/0.5 min. Essentially the same curves were obtained in the cooling process. The observed absorbance has been normalized at 60 °C. Inset is the van't Hoff plots of the corresponding melting curves.

Table 1. List of the T_m Values and Thermodynamic Parameters for O(A_n)−d(T_n) Hybrids

n	T_m (°C)	$\Delta H/n$ (kcal residue mol^{-1})	$\Delta S/n$ (cal residue mol^{-1} K^{-1})
6	14 ± 1[a]	−10 ± 2[a]	−31 ± 7[a]
9	35	−11	−35
12	45	−12	−34
15	51	−13	−37

[a] Large error is due to uncertainty in low-temperature-side baseline and the nonlinear van't Hoff plot.

the same, irrespective of the chain lengths and that the structure is nearly optimized for the hybridization.

The thermodynamic parameters obtained from the van't Hoff plots have been known to contain errors that mainly originate from the uncertainty in taking baselines at the high- and low-temperature sides.[8] Reliable thermodynamic parameters can be obtained from the concentration dependence of the melting temperatures by using eq 1.[8]

$$1/T_m = (2.303R/\Delta H)\log(c/2) + \Delta S/\Delta H \qquad (1)$$

The melting curves of the o(A_9)−d(T_9) hybrids were measured at different concentrations from c = [o(A_9)]$_0$ = [d(T_9)]$_0$ = 2.5×10^{-8} to 2.5×10^{-5} mol L^{-1}. It was found that the $1/T_m$ versus log $c/2$ plot consisted of two linear parts, one being at the low concentration side from 2.5×10^{-8} to 5×10^{-7} mol L^{-1} and the other being at the high concentration side from 5×10^{-7} to 2.5×10^{-5} mol L^{-1}. The slope of the low concentration side gave $\Delta H/9 = -11$ kcal mol^{-1} and $\Delta S/9 = -36$ cal mol^{-1} K^{-1}, that are in good agreement with those from the melting curves. However, the slope of the high concentration side gave $\Delta H = -7.0$ kcal mol^{-1} and $\Delta S = -21$ cal mol^{-1} K^{-1} that are markedly deviated from the former values. Similar discrepancy was observed for other o(A_n)−d(T_n) hybrids and for the Nielsen-type PNA(A_n)−d(T_n) hybrids, when they are hybridized under moderately high concentrations. In contrast, this type of discrepancy was not observed for the d(A_n)−d(T_n) hybrids. The discrepancy may be interpreted in terms of the self-association of the OPNA and PNA molecules or in terms of the imperfect duplex formation[9] at moderately high concentrations. Detailed discussion on this subject will be made in a future report.

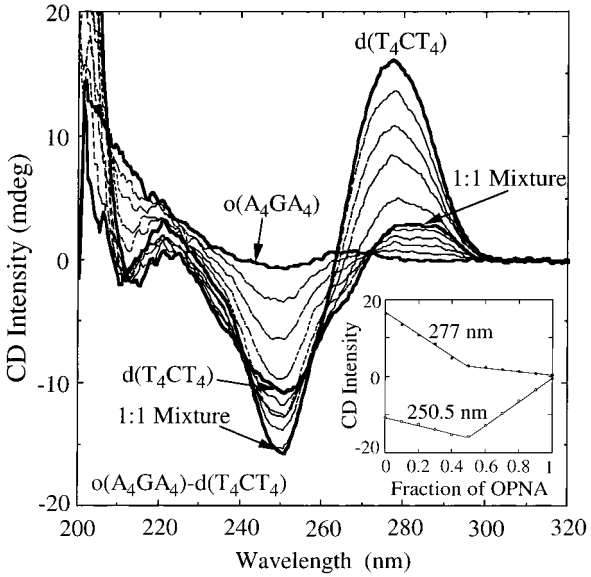

Figure 2. CD spectra of o(A_4GA_4)−d(T_4CT_4) mixtures with different OPNA/DNA ratios. Inset is Job plots for CD intensities at 250.5 and 277 nm. [o(A_4GA_4)] + [d(T_4CT_4)] = 1.0×10^{-5} M, in 1 M NaCl, 10 mM NaH_2PO_4, 0.1 mM EDTA at pH = 7.0, 5 °C.

Stoichiometry and Relative Stabilities of Hybrids of o(A_4NA_4)−d($T_4N'T_4$). To examine the compatibility of other base pairs in the OPNA−DNA hybrids, o(A_4NA_4)s with N = A, G, C, U, or X (abasic), were synthesized. CD spectra were measured for various o(A_4NA_4)−d($T_4N'T_4$) mixtures under different OPNA/DNA ratios. Figure 2 shows CD spectra of the o(A_4GA_4)−d(T_4CT_4) mixtures. The CD spectra shows two types of isodichroic points; the first type at 271 nm appeared when [OPNA] > [DNA] and the second type at 241 and 258 nm appeared when [OPNA] < [DNA]. The first type of isodichroic point indicates that the mixture with excess OPNA contains only the 1:1 hybrid and free OPNA. Similarly, the second type of isodichroic points indicates that the mixture with excess DNA contains only the 1:1 hybrid and free DNA. The CD Job plot in the inset supports the 1:1 stoichiometry of the hybridization. The two straight lines that are crossing at the 1:1 ratio indicate that no component other than the 1:1 duplex is formed in the OPNA−DNA mixture.

Similar CD spectra with two-types of isodichroic points were observed in other o(A_4NA_4)−d($T_4N'T_4$) mixtures with the complementary N−N′ pairs. In all complementary pairs, a 1:1 stoichiometry was confirmed from the CD Job plot. These CD data indicate that OPNAs form only duplex hybrids with the complementary DNAs, and no other species is present in the system.

Stabilities of Complementary and Noncomplementary Base Pairs in the OPNA−DNA Hybrids. To evaluate the stabilities of all possible combinations of base pairs in the OPNA−DNA hybrids, the melting curves of the o(A_4NA_4)−d($T_4N'T_4$) hybrids were measured, where N represents A, G, U, C, or X (abasic) and N′ represents T, C, A, or G. The melting temperatures obtained are collected in Table 2. The melting curve of the o(A_4GA_4)−d(T_4CT_4) hybrid is shown in Figure 3 (open circles). Again, the melting curve was reversible in the

(8) Puglisi, J. D.; Tinoco, I., Jr. *Methods Enzymol.* **1989**; *180*, 304.

(9) Wu, P.; Sugimoto, N. *Nucleic Acids Res.* **2000**, *28*, 4762.

Table 2. T_m Values (°C) for Various o(A_4NA_4)−d($T_4N'T_4$) Hybrids

N in o(A_4NA_4)	N′ in d($T_4N'T_4$)			
	T	C	A	G
A	35	17	17	15
G	nd[b]	35	14	15
U	nd[b]	19	20	16
C	nd[b]	15	16	23
X[a]	nd[b]	12	15	14

[a] Abasic unit. [b] Melting temperature could not be determined due to a two-step transition.

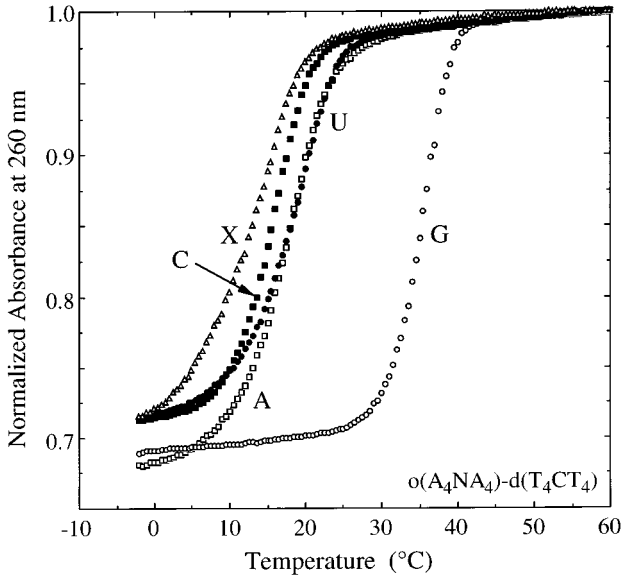

Figure 3. Temperature dependence of absorption intensity at 260 nm for equimolar mixtures of o(A_4NA_4)−d(T_4CT_4) with N = A, G, C, U, and X (abasic). Other conditions are the same as Figure 1.

heating and cooling processes and shows a very sharp transition at T_m = 35 °C. When a single mismatch was introduced in the middle of the 9-base pair hybrids of o(A_4NA_4)−d(T_4CT_4), the T_m values lowered by more than 16 °C **(**Figure 3**)**. The high T_m value for the full-match pair of o(A_4GA_4)−d(T_4CT_4) and the significant lowering of the T_m values for the single mismatch hybrids suggest that the structure of the G-C pair in the OPNA−DNA hybrid is also close to the optimum for the hybridization.

Similar study was carried out on the o(A_4NA_4)−d(T_9) hybrids. The melting curves are shown in Figure 4. The T_m value of the full-match hybrid (35 °C) is higher than other hybrids that contain a single mismatch. The melting curves of the mismatch hybrids, however, show exceptionally high T_m values as compared with other mismatch hybrids and also show two-step transitions. The two-step transition is not due to an intrinsic property of o(A_4NA_4), because no such phenomenon has been observed when they were hybridized with other DNAs of full-match and single-mismatch sequences. Since the two-step transition was observed both in the heating and cooling processes, the OPNA/DNA mixture must be converted from the single-stranded form at high temperatures to an intermediate hybrid at medium temperatures and finally to a stable hybrid at low temperatures.

The two-step transition of the o(A_4NA_4)−d(T_9) hybrids might be explained in terms of very flexible nature of the OPNA chain. If the OPNA chain is flexible enough, a read-through of a noncomplementary base of OPNA would take place, leading to a hybridization between the A_8 part of o(A_4NA_4) and the T_8 part of d(T_9), as illustrated in Figure 5 (1). This type of read-

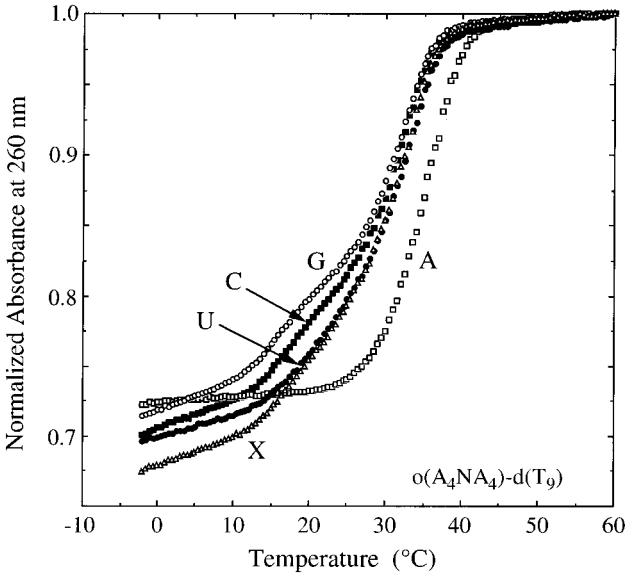

Figure 4. Temperature dependence of absorption intensity at 260 nm for equimolar mixtures of o(A_4NA_4)−d(T_9) with N = A, G, C, U, and X (abasic). Other conditions are the same as Figure 1.

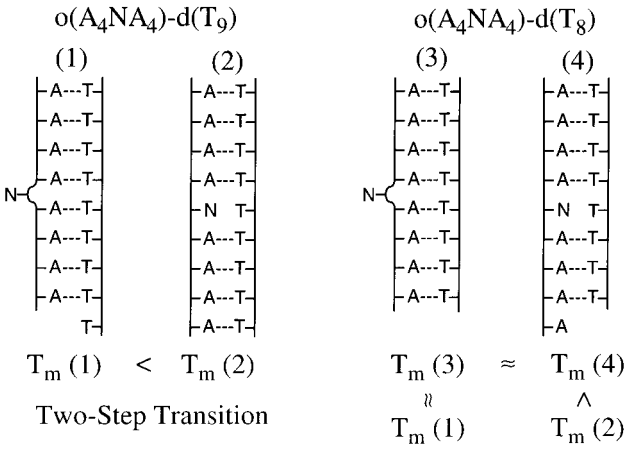

Figure 5. Possible mechanism for the two-step melting of the o(A_4NA_4)−d(T_9) and o(A_4NA_4)−d(T_8) hybrids (N ≠ A).

through can take place only in the o(A_4NA_4)−d(T_9) hybrids. To test this possibility, melting curves of the o(A_4NA_4)−d(T_8) 1:1 mixture were measured. The stability of the read-through would not be changed by changing the partner from d(T_9) (1) to d(T_8) (3), but the stability of the normal configuration will be reduced by the partner change from (2) to (4). Therefore, the partner change will result in the disappearance or the decrease of the higher T_m values and the invariance of the lower T_m values.

Melting curves of the o(A_4UA_4)−d(T_9) and o(A_4CA_4)−d(T_9) are compared with those with d(T_8) as the partner in Figure 6. As predicted above, the melting curve with d(T_8) shows a single-step transition in the case of o(A_4UA_4), and becomes close to a single-step one in the case of o(A_4CA_4). Similarly, the melting curve for the o(A_4GA_4)−d(T_8) pair was close to the single-step one. These data support the read-through configuration in the case of o(A_4NA_4)−d(T_9) pairs.

Melting curves of the o(A_4NA_4)−d(T_4AT_4) series also showed sharp transitions, and the melting temperatures are collected in Table 2. The highest T_m value (20 °C) was observed for the complementary hybrid, o(A_4UA_4)−d(T_4AT_4), but it is significantly lower than that of the complementary hybrids of o(A_9)−d(T_9) (35 °C) and o(A_4GA_4)−d(T_4CT_4) (35 °C). Simi-

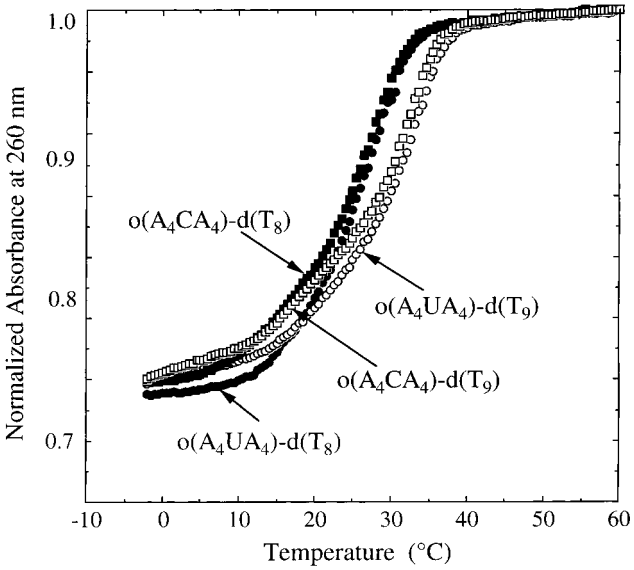

Figure 6. Comparison of the melting curves of the o(A_4NA_4)−d(T_9) and o(A_4NA_4)−d(T_8) hybrids (N = U and C).

larly, the complementary hybrid, o(A_4CA_4)−d(T_4GT_4), showed the highest T_m value among the o(A_4NA_4)−d(T_4GT_4) series, but it is not high enough (23 °C). These data indicate that the structures of the complementary base pairs in the o(A_4-pyrimidine-A_4)−d(T_4-purine-T_4) series do not match perfectly to each other. The T_m values further decreased when two or more pyrimidine units were incorporated into OPNA. However, as will be described below, a 12-mer OPNA incorporated with three C units still showed a fairly high T_m value (26 °C) when it is hybridized with the complementary DNA.

To understand the effect of a mismatch in the o(A_4NA_4)−d($T_4N'T_4$) hybrids, an abasic unit (X) was introduced in the middle of the OPNA. The melting temperatures of o(A_4XA_4)−d($T_4N'T_4$) are listed in Table 2. Since no structural overlapping is expected for X−N′ pairs, all o(A_4XA_4)−d($T_4N'T_4$) hybrids must show similar melting temperatures, irrespective of the N′ units. Actually, this is the case for N′ = A, C, and G. Furthermore, these melting temperatures are not much different from those of the o(A_4NA_4)−d($T_4N'T_4$) hybrids with mismatch N−N′ pairs. This indicates that the mismatch base pair is simply ignored without affecting the whole configuration of hybrids significantly. In the case of o(A_4XA_4)−d(T_9) hybrid, a two-step transition was observed, indicating the read-through of the X−T pair is taking place.

Melting curves of the complementary OPNA−DNA hybrids are compared with those of the DNA−DNA hybrids in Figure 7. The OPNA−DNA hybrids show higher T_m values and sharper transitions than the DNA−DNA hybrids. Hybrids between the OPNAs of purine bases and the DNAs of pyrimidine bases are much more stable than other cases. Because of the limited application of the purine-rich sequences in the Nielsen-type PNA, the purine-rich sequences of OPNA will find applications as the substitute of the Nielsen-type PNA.

A similar sharp transition was also observed for the o(A_{12})-RNA(U_{12}) hybrid, although the melting temperature was lower than that of the OPNA−DNA hybrid. The T_m value was 18.5 °C, and the temperature range for the 5−95% transition was 15 °C.

CD Spectroscopic Information on the Structures of the OPNA−DNA Hybrids. CD spectra of the complementary hybrids of o(A_4NA_4)−d($T_4N'T_4$) at 10 °C are compared in Figure 8. CD profile of the o(A_4CA_4)−d(T_4GT_4) hybrid is

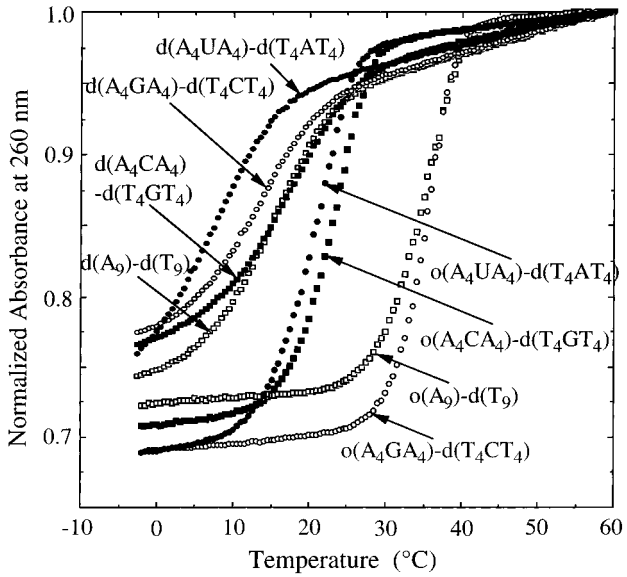

Figure 7. Melting curves of the complementary hybrids of o(A_4NA_4)−d($T_4N'T_4$) pairs and d(A_4NA_4)−d($T_4N'T_4$) pairs [N, N′ = A, G, U(T), C].

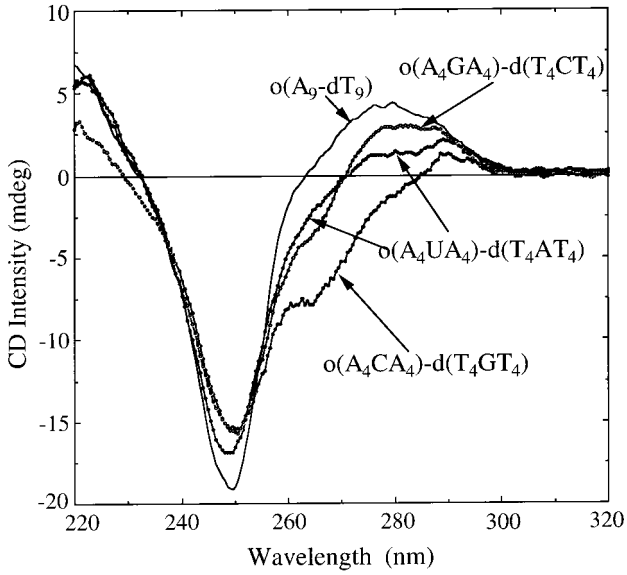

Figure 8. CD spectra of the complementary hybrids of o(A_4NA_4)−d($T_4N'T_4$) pairs [N, N′ = A, G, U(T), C]. Conditions of CD measurement are the same as Figure 2.

significantly different from that of the o(A_9)−d(T_9) hybrid. The large difference cannot be attributed to the insertion of a single o(C)−d(G) pair but suggests a conformational change of the whole hybrid caused by a less compatible o(C)−d(G) pair. The CD result is inconsistent with the reduced stability of this complementary hybrid. The CD change was smaller, however, in the o(A_4UA_4)−d(T_4AT_4) hybrid that also showed a reduced stability. The CD profile of the o(A_4GA_4)−d(T_4CT_4) hybrid also showed a small change that may be attributed to the insertion of the o(G)−d(C) pair. The CD data, although not conclusive, may suggest that the relative stabilities of the complementary hybrids are mainly determined by the extent of their conformational deviation from the optimized conformation of the o(A_9)−d(T_9) hybrid.

Direction of the OPNA−DNA Hybrids. So far, only symmetrical sequences have been used in order to focus on the relative stabilities of different base pairs. However, OPNA may prefer one of the two directions in hybridizing with DNAs, that

is, N(amino end) to C′(carboxyl end) with 5′ to 3′ (parallel) or N to C′ with 3′ to 5′ (antiparallel). Incidentally, the Nielsen-type PNA prefers antiparallel direction, although less stable hybrids are formed in parallel direction. The melting temperature of the o(A_5CAACACA)−d(5′-T_5GTTGTGT-3′) parallel hybrid (26 °C) was higher than that of the o(A_5CAACACA)−d(5′-TGTGTTGT$_5$-3′) antiparallel hybrid (15 °C). Higher T_m was also observed in the o(A_5GAAGAGA)−d(5′-T_5CTTCTCT-3′) parallel hybrid (24 °C) than in the o(A_5GAAGAGA)−d(5′-TCTCTTCT$_5$-3′) hybrid (20 °C). Both data indicate that OPNAs prefer parallel hybridization with DNAs, in contrast to the Nielsen-type PNAs.

Conclusions

OPNAs with mixed sequences were synthesized through conventional solid-phase technique. No difficulty was found in synthesizing any base sequences, particularly the purine-rich sequences. The o(A_n)−d(T_n) hybrids showed higher T_m values for longer chains up to $n = 15$, indicating that the structure of o(A_n) is nearly optimized for the hybridization with d(T_n). The effect of the types of base pairs was examined for o(A_4NA_4)−d(T_4N′T_4) hybrids that contain various (N−N′) pairs. All complementary hybrids showed higher T_m values than the hybrids that contained a single mismatch, indicating all base pairs are correctly recognized in the hybrids. The mismatch base pairs may be ignored in the hybrids, since they behave similarly to the X(abasic)-N′ pairs. The complementary OPNA−DNA hybrids showed higher T_m values and sharper transitions than the DNA−DNA hybrids. The OPNA−DNA hybrids prefer parallel direction. These data suggest possible applications of OPNAs as antisense/antigene drugs and diagnostic devices, particularly for purine-rich sequences.

Acknowledgment. This work has been supported by a Grand-in-Aid for Specially Promoted Research from the Ministry of Education, Science, Sports and Culture, Japan (No. 11102003).

Supporting Information Available: Experimental details of the synthesis of abasic OPNA unit and the synthesis and characterization of OPNAs with mixed sequences (PDF). This material is available free of charge via the Internet at http://pubs.acs.org.

JA003881I